

Higgs Recoil Mass and Higgs-Strahlung Cross-Section Study for the ILD LOI

Hengne LI

Laboratoire de l'Accélérateur Linéaire (LAL),
91898 Orsay Cedex, France

Laboratoire de Physique Subatomique et de Cosmologie (LPSC),
38026 Grenoble Cedex, France

This proceeding summarizes the Higgs recoil mass and Higgs-strahlung cross-section study done for the Letter of Intent (LOI) of the International Large Detector (ILD) Concept. Assuming $M_H = 120$ GeV, working at $\sqrt{s} = 250$ GeV with beam parameters RDR250 and beam polarization $P(e^-, e^+) = (-80\%, +30\%)$, this full simulation study predicts that, the ILD detector can achieve 37 MeV precision on the M_H measurement and 3.3% on the cross-section measurement from the $ZH \rightarrow \mu^+\mu^-X$ channel, while 83 MeV and 4.9% from the $ZH \rightarrow e^+e^-X$ channel, if we have 250 fb^{-1} integrated luminosity.

1 Introduction

Experimental conditions at the proposed International Linear Collider [1] (ILC) provide an ideal environment for the precision studies of Higgs production own to the unparalleled cleanliness and well-defined initial conditions. We can use the Higgs-strahlung process ($e^+e^- \rightarrow Z^* \rightarrow ZH$), which is a major Higgs production mechanism at the ILC, to precisely measure the Higgs mass (M_H) independent of its decay modes, using the mass recoiling to the Z boson, with $Z \rightarrow \mu^+\mu^-$ or e^+e^- . The major advantage of this recoil mass method is we do not need any information about how the Higgs decays. To calculate the M_H , we only need the Z boson reconstructed from the lepton pair it decays with the precisely known center of mass energy (\sqrt{s}). We can also precisely determine the Higgs-strahlung cross-section (σ) and therefore the coupling strength at the HZZ vertex, without any bias from the Higgs decay assumptions.

This proceeding summarizes the Higgs recoil mass and Higgs-strahlung cross-section study done for the Letter of Intent [4] (LOI) of the International Large Detector [2] (ILD) Concept. It is a most realistic full simulation study up to now based on the ILC design issued in the ILC Reference Design Report [3] (RDR) and the ILD detector concept. Thus, it has contemplated all the major effects we have thought of from both the accelerator and the detector. It assumes $M_H = 120$ GeV, the ILC works at $\sqrt{s} = 250$ GeV, and an integrated luminosity of 250 fb^{-1} (equivalent to four years of data taking). The study also assumes two options of beam longitudinal polarization, $e_L^-e_R^+$: ($e^- : -80\%$, $e^+ : +30\%$) and $e_R^-e_L^+$: ($e^- : +80\%$, $e^+ : -30\%$), to quantitatively estimate the benefits from the beam polarization.

The results of this study are published in the ILD LOI, with an accompany physics note [5] summarizing the methods. For the complete documentation of this study, please refer to my Ph.D thesis [6].

2 Production

The event generation is centrally done at SLAC [7] using WHIZARD [8] v1.40, based on a detailed beam simulation using GUINEA-PIG [9] with beam parameters given in ILC RDR, in which the beam energy spread are 0.28% and 0.18% for electron and positron beams, respectively. Both the Initial-State Radiation (ISR) and Final-State Radiation (FSR) are included in the event generation. The full simulation of the ILD detector and the reconstruction are done at DESY and KEK using software package ILCSoft [10] v01-06.

Table 1 give the cross-sections of signal and major backgrounds considered in this study. We categorize the backgrounds according to the final states. For instance, the ee background consists of $e^+e^- \rightarrow Z/\gamma^* \rightarrow e^+e^-$, the $\mu\nu\mu\nu$ background is mostly the $WW \rightarrow \mu\nu\mu\nu$, but also $ZZ \rightarrow \mu\nu\mu\nu$, while the $eeff$ background comes from all the possible intermediate states $e^+e^- \rightarrow Z/\gamma^*Z/\gamma^*$.

Process	Cross-Section		Process	Cross-Section	
	$e_L^-e_R^+$	$e_R^-e_L^+$		$e_L^-e_R^+$	$e_R^-e_L^+$
$\mu\mu X$	11.67 fb	7.87 fb	$ee X$	12.55 fb	8.43 fb
$\mu\mu$	10.44 pb	8.12 pb	ee	17.30 nb	17.30 nb
$\tau\tau$	6213.22 fb	4850.05 fb	$\tau\tau$	6213.22 fb	4814.46 fb
$\mu\nu\mu\nu$	481.68 fb	52.37 fb	$e\nu e\nu$	648.51 fb	107.88 fb
$\mu\mu ff$	1196.79 fb	1130.01 fb	$ee ff$	4250.58 fb	4135.97 fb

Table 1: Cross-sections with the two options of beam polarization $e_L^-e_R^+$ and $e_R^-e_L^+$. The signal is indicated by bold face letters.

3 Event Selection

The first step in the event selection is the identification of leptonically decaying Z bosons. We require the lepton tracks to be well measured by removing tracks with large uncertainties on the reconstructed momentum. The efficiency to identify a pair of leptons from the decay of a Z boson is 95.4 % for $Z \rightarrow \mu^+\mu^-$ and 98.8 % for $Z \rightarrow e^+e^-$.

The second step in the event selection is to suppress the backgrounds who also have a pair of leptons identified. We can suppress most of them using some common kinematic requirements. These requirements are, the invariant mass of the lepton pair (M_{dl}) is around the Z boson mass, a large transverse momentum (P_{Tdl}) of the lepton pair, a not-so-forward polar angle ($\cos\theta_{dl}$) distribution of the lepton pair system, the pair of leptons is not back-to-back (acoplanarity), and a restrict on the recoil mass (M_{recoil}) window around the Higgs mass.

There are irreducible backgrounds like lepton pairs ($\mu\mu$ or ee), WW and ZZ after the requirements above.

For the irreducible lepton pair background, we have found another method named P_T balance. The idea is to identify the energetic ISR photons, and ask them to balance the P_T of the lepton pair. We can observe a great P_T balance from the lepton pair background, while not from the ZH signal. This is because, the irreducibility of the lepton pair backgrounds is owen to the fact that the ISR energy loss reduces the effective \sqrt{s} , thus migrates them to the acceptable window of our common kinematic requirements. Together with a veto of the

photon conversions by requiring a large polar angle difference between the pair of leptons, we can totally remove the lepton pair backgrounds.

For the irreducible WW and ZZ backgrounds, we employ a Likelihood method for the further suppression. We use variables M_{dl} , P_{Tdl} , $\cos\theta_{dl}$ and acollinearity to build the templates for Likelihood calculation, and optimize the cut on the Likelihood according to the maximum of the significance. The Likelihood further suppression rejects the WW and ZZ backgrounds further by one half.

With this event selection scenario, we can keep an efficiency of around 55 % with a signal over background ratio of about 4 under the recoil mass peak for the $ZH \rightarrow \mu\mu X$ channel.

4 Fitting Methods

After the event selection, the remaining spectrum consists of the ZH signal (S) and the irreducible backgrounds (B). Now we need to build a composed model $F_M(x; M_H, N_S) = N_S \cdot F_S(x; M_H) + N_B \cdot F_B(x)$, and fit it to the remaining spectrum to extract our results. In the composed model, the M_H and N_S are the free parameters we need to determine. M_H is the Higgs mass, and the N_S is for the calculation of the cross-section.

We choose the polynomial function to describe the shape of the background. For the signal, I have studied three functions in my thesis. They are:

- Use Gaussian to describe the Peak and adding an Exponential to complement the Tail (GPET). It is function modified from previous contributions [12, 11]. My modification makes both itself and its first derivative being continuous.
- An implementation of the Kernel Estimation [13] using Gaussian kernel.
- A Physics Motivated function first developed in my thesis. The development started from Yokoya-Chen's Beamstrahlung approximation [14, 15, 16, 17], analytically convoluted with the ISR approximation [18]. After a numerical convolution with the Gaussian function, I propagated it to the recoil mass. With this Physics Motivated function, and known the beam parameters, I can essentially predict the generator level ZH spectrum.

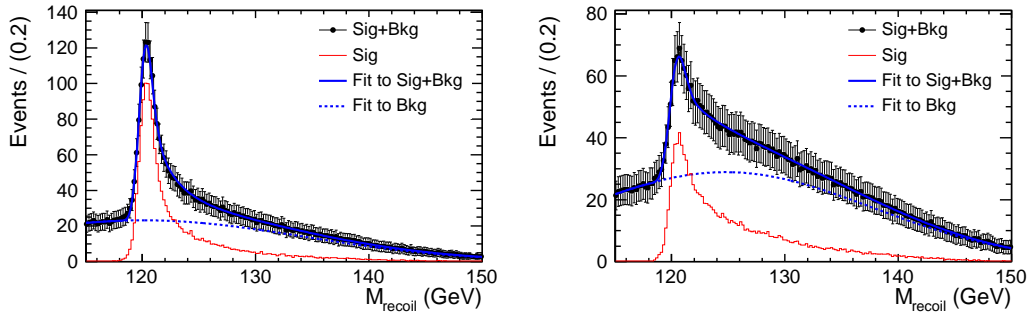


Figure 1: Fits using the Physics Motivated function to describe the signal, for $ZH \rightarrow \mu\mu X$ (Left) and eeX (Right) channels, taking beam polarization $e_L^- e_R^+$ as examples.

Figure 1 shows the fits using the Physics Motivated function to describe the signal, for both the $ZH \rightarrow \mu\mu X$ and eeX channels, taking beam polarization $e_L^- e_R^+$ as examples. The precisions derived from the fits are 37 MeV on the M_H measurement and 3.3 % on the σ measurement from the $\mu\mu X$ channel, while 83 MeV and 4.9 % from the eeX channel.

5 Bremsstrahlung Recovery

The results derived above shows the eeX channel gives almost twice the errors on both the M_H and the σ measurements, than those from the $\mu\mu X$ channel. This is because the electrons suffer heavily from the Bremsstrahlung energy loss, reminding that the ILD detector has about 4 % X_0 material budget before TPC.

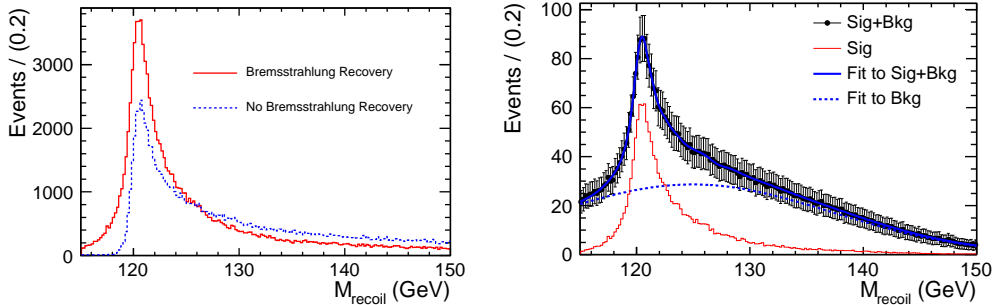


Figure 2: Left: Comparison of the recoil mass distributions with and without Bremsstrahlung recovery. Right: Fit of the eeX channel with Bremsstrahlung recovery corresponding to that in Figure 1.

A dedicated algorithm [19] is employed in this study to identify the Bremsstrahlung photons and merge them into the Z boson. Figure 2 (Left) shows a comparison of the Higgs recoil mass spectra with and without Bremsstrahlung recovery. We can observe the Bremsstrahlung recovery significantly increases the statistics while degrades the mass resolution because of the worse ECAL energy resolution for low energy photon reconstruction.

Figure 2 (Right) shows the fit of the eeX channel with Bremsstrahlung recovery corresponding to that in Figure 1. The results with Bremsstrahlung recovery are 73 MeV on the M_H measurement (~ 10 % improvement), and 3.9 % on the σ measurement. With the Bremsstrahlung recovery, the accuracy of the M_H measurement is still worse than that of the $\mu\mu X$ channel by a factor of two. However, the accuracy of the cross section measurement becomes similar to that of the $\mu\mu X$ channel, since it is less sensitive to the mass resolution.

6 Results

Table 2 summarizes the resulting precisions of the measurements for both beam polarization $e_L^- e_R^+$ and $e_R^- e_L^+$, where those of the eeX have Bremsstrahlung recovered, and the “merged” means the results by combining the two leptonic channels.

Pol.	Ch.	M_H (GeV)	σ (fb)
$e_L^- e_R^+$	$\mu\mu X$	120.001 ± 0.037	11.63 ± 0.39 (3.35%)
	eeX	119.997 ± 0.073	12.52 ± 0.49 (3.91%)
	merged	120.006 ± 0.033	12.02 ± 0.31 (2.54%)
$e_R^- e_L^+$	$\mu\mu X$	119.997 ± 0.040	7.82 ± 0.28 (3.58%)
	eeX	120.003 ± 0.081	8.41 ± 0.36 (4.28%)
	merged	120.005 ± 0.035	8.09 ± 0.22 (2.73%)

Table 2: Resulting Higgs mass M_H and cross section σ , of the $\mu\mu X$ channel and eeX channel with Bremsstrahlung recovery. The “merged” means the results by combining the two leptonic channels.

7 Conclusion

The results in Table 2 shows the best results of a single leptonic channel come from $ZH \rightarrow \mu\mu X$. Even including the Bremsstrahlung recovery, the eeX channel gives worse results than the $\mu\mu X$ channel by a factor of two in the M_H measurement, and by a factor of 1.5 in the σ measurement. This is because of the worse energy resolution of the soft photon measurement by the ECAL, and larger backgrounds related to eeX channel.

The results with beam polarization $e_L^- e_R^+$ are better than those of the $e_R^- e_L^+$ by about 10 %. The reasons are that, although the polarization $e_R^- e_L^+$ suppresses the WW background, the cross sections of the Higgs-strahlung process are smaller by about 20 % compared to that of the polarization $e_L^- e_R^+$. At the same time, the methods we have developed are efficient enough for the suppression of the WW background. Hence the polarization $e_L^- e_R^+$ gives better results.

We may also conclude that there are two accelerator effects, the beam energy spread and the Beamstrahlung, have great impact on Higgs recoil mass measurement. The beam energy spread increases the width of the recoil mass peak, thus reduces the accuracy of the mass measurement. The Beamstrahlung largely reduces the effective statistics on the recoil mass peak.

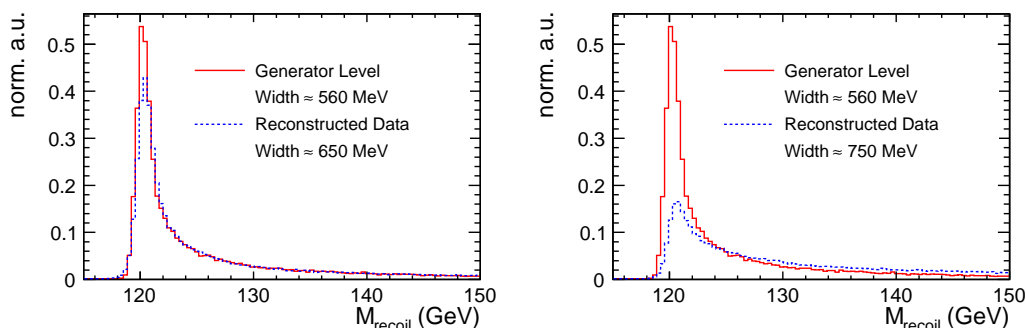


Figure 3: The Higgs recoil mass distributions in the $\mu\mu X$ channel (Left) and eeX channel (Right), comparison of those before and after detector simulation.

Figure 3 compares the Higgs recoil mass distributions before (generator level) and after (reconstructed) full detector simulation and reconstruction for $\mu\mu X$ channel (Left) and eeX channel (Right). The distribution in the generator level has the accelerator effects imposed, while that after reconstruction has the detector effects added.

For the recoil mass distributions of $\mu\mu X$ -channel, a fit to the left side of the maximum using a Gaussian function gives the mass resolutions to be 560 MeV in the generator level, and 650 MeV after full detector simulation. The detector response leads to a broadening of the recoil mass maximum from 560 MeV to 650 MeV. The contribution from the uncertainty of detector response is therefore estimated to be 330 MeV. This observation indicates that *the dominant contribution to the observed width of the $\mu\mu X$ recoil mass distribution arises from the incoming beams rather than the response of the ILD detector.*

8 Outlook

All what we have intensively studied in the past is how to reduce the statistical errors on these two measurements. A serious study of the systematic errors is apparently missing in the context.

In the Higgs recoil mass measurement, the systematic biases appear as the difference between the measured value and the true value. Observables correlated with the Higgs recoil mass are the center of mass energy and the momenta of the pair of leptons. Imperfect knowledge of these variables could introduce systematic bias to the Higgs recoil mass measurement. To control them, a well studied reference reaction is needed.

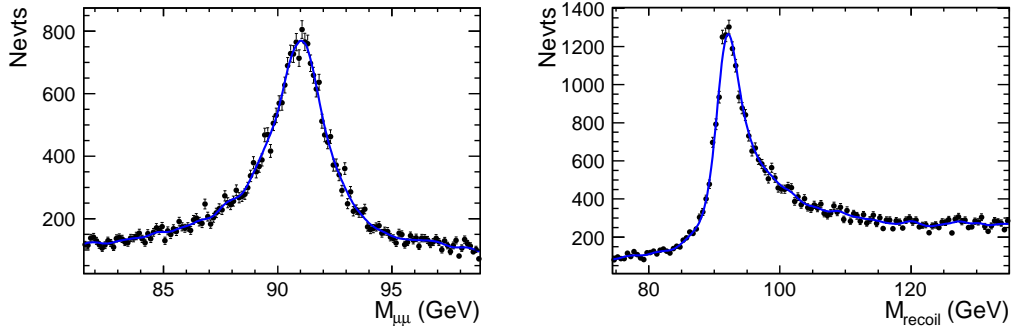


Figure 4: Fit of the *Invariant Mass* (Left) and *Recoil Mass* (Right) of the $Z \rightarrow \mu^+ \mu^-$ in the ZZ process using *Kernel Estimation*, with polarization mode $e_L^- e_R^+$. An accuracy of 13 MeV is obtained for the invariant mass measurement, and 28 MeV for the recoil mass measurement.

The ZZ process is an excellent choice, with the M_Z precisely known to a precision of 2 MeV [20]. The ZZ process has a similar scenario as the Higgs-strahlung process with one Z boson decays to a pair of muons or electrons, and the recoil mass of the Higgs replaced by that of the other Z boson.

By measurement of the invariant mass of the $Z \rightarrow l^+ l^-$, the tracking momentum measurement can be calibrated. At $\sqrt{s} = 250$ GeV, assuming $M_H = 120$ GeV, the $ZZ \rightarrow \mu\mu X/eeX$ has about 40 times larger cross section than that of the $ZH \rightarrow \mu\mu X/eeX$.

With this much larger statistics the Z mass can be measured to a precision of 13 MeV, using channel $ZZ \rightarrow \mu\mu X$, see Figure 4 (Left) for the fit.

The Z recoil mass of the ZZ process can be used to determine and control the center of mass energy and the radiative effects. The Z recoil mass could be determined to a statistical precision of 28 MeV, using channel $ZZ \rightarrow \mu\mu X$, see the fit in Figure 4 (Right). With this small statistical error, the knowledge of the center of mass energy and the radiative effects could be validated precisely.

On the cross-section measurement, the major systematic error comes from the uncertainty of the efficiency. The procedure to measure the uncertainty of the efficiency is to vary the physics assumptions together with the various background rejection methods to estimate the dependences and covariances between them. Reminding we applied a very complicated background rejection method. The complicated background rejection mandatorily introduces more difficulties in the measurement of the uncertainty of the efficiency.

For the cross section measurement, we found that the statistical error does not request such a high suppression of the background as for the mass measurement. By removing the Likelihood method and remaining only cuts on some basic variables M_{dl} , P_{Tdl} , and P_T balance, the statistical error on the cross section measurement only increases by about 10 % on average. This means a similar statistical error could be obtained with much less sources of systematic error due to the background rejection methods.

References

- [1] International Linear Collider, <http://www.linearcollider.org/> (2009)
- [2] International Large Detector concept, <http://www.ilcild.org/> (2009)
- [3] ILC Reference Design Report, <http://www.linearcollider.org/about/?pid=1000437> (2007)
- [4] *ILD Letter of Intent*, <http://www.ilcild.org/documents/ild-letter-of-intent> (2009)
- [5] H. Li, *et. al.*, LAL-09-121, LC-PHSM-2009-006, (2009)
- [6] H. Li, Ph.D. Thesis, Université de Paris-Sud XI, LAL-09-118, (2009)
- [7] SLAC Standard Model Data Samples, (2009)
<https://confluence.slac.stanford.edu/display/ilc/Standard+Model+Data+Samples>
- [8] W. Kilian, T. Ohl, and J. Reuter, <http://whizard.event-generator.org/> , (2009)
- [9] D. Schulte, GUINEA-PIG, Ph.D. Thesis, University of Hamburg, (1996)
- [10] ILC Software, <http://ilcsoft.desy.de/> (2009)
- [11] P. Garcia-Abia, W. Lohmann, Eur. Phys. J. direct C2:2 (2000)
- [12] M. Ohlerich, *et. al.*, LCWS07 Proc. Vol. 1, p. 159-165 (2007)
- [13] K. S. Cranmer, *Kernel estimation in High-energy physics*, Comput. Phys. Commun. **136** (2001) 198, hep-ph/0005309
- [14] Y. Yokoya and P. Chen, *Frontiers of Particle Beams: Intensity imitations*, Springer-Verlag, (1992)
- [15] P. Chen, Phys. Rev. D **46**, 1186 (1992)
- [16] P. Chen, T.L. Barklow and M.E. Peskin, Phys. Rev. D **49**, 3209 (1994)
- [17] M.E. Peskin, SLAC-TN-04-032, LCC-0010 (1999)
- [18] F.A. Berends, R. Kleiss and S. Jadach, Nucl. Phys. **B202** (1982) 63; Computer Physics Commun. **29** (1983) 185
- [19] M.A. Thomson, *ZFinder: A Marlin processor for Bremsstrahlung recovery.*, (2009)
- [20] Particle Data Group, *Review of Particle Physics*, Physics Letters **B667**, 1 (2008)